Toughening of Unsaturated Polyester Resins with Core–Shell Rubbers

Yan-Jyi Huang, Jia-Horng Wu, Jiing-Guan Liang, Mann-Wen Hsu, Jiun-Kwei Ma

Department of Chemical Engineering, National Taiwan University of Science and Technology, Taipei, Taiwan 106, Republic of China

Received 2 October 2005; accepted 15 May 2006
DOI 10.1002/app.25159
Published online 28 September 2007 in Wiley InterScience (www.interscience.wiley.com).

ABSTRACT: The effects of core–shell rubbers (CSRs) as tougheners on the fracture properties of unsaturated polyester (UP) resins during curing at 110°C are investigated. CSRs were synthesized by two-stage soapless emulsion polymerizations; the soft core was made from rubbery poly(*n*-butyl acrylate), whereas the hard shell was made from methyl methacrylate, ethylene glycol dimethacrylate, and various concentrations of glycidyl methacrylate. Depending on the content of glycidyl methacrylate in the CSR shell and the amount of CSR added to the UP, the fracture properties of the CSR-toughened UP resins varied. The experimental results are explained by an integrated approach of measurements of the static phase characteristics of a styrene/UP/CSR system, the reaction kinetics, the cured sample morphology, the glass-transition temperatures, and the fracture toughness with differential scanning calorimetry, scanning electron microscopy, transmission electron microscopy, and dynamic mechanical analysis. Finally, the toughening mechanism for the CSR-toughened UP resins is also explored. © 2007 Wiley Periodicals, Inc. J Appl Polym Sci 107: 939–950, 2008

Key words: emulsion polymerization; resins; rubber

INTRODUCTION

Unsaturated polyester (UP) resins are the most widely used thermoset resins in polymer processing.[1] However, cured UP resins usually exhibit high polymerization shrinkage, which is due to the extensive intramolecular reactions of UPs during the cure, and poor resistance to crack propagation, which is due to their brittleness. The former drawback can be solved by the addition of low-profile additives (LPAs)[2] to UP, whereas the latter problem can be remedied by the addition of tougheners.[3–7]

To improve the toughness of cured UP resins, most researchers[4–7] have employed specific reactive liquid rubbers, that is, butadiene–acrylonitrile copolymers containing terminal functional groups such as carboxyl, amine, acrylic, mercaptan, and hydroxyl groups, to increase the interfacial adhesion between the tougheners and UP resins during the cure. Although different degrees of success have been achieved, liquid rubber-modified UP resins inevitably cause a profound decrease in the mechanical modulus and glass-transition temperature for molded parts. In contrast, core–shell rubbers (CSR)[3,8] with rubbery-type materials as a core have been recently employed to toughen epoxy resins and vinyl ester resins without a significant reduction of the thermomechanical properties.

The objective of this work is to study the effects of CSR tougheners, with poly(butyl acrylate) (PBA) as the core and poly(methyl methacrylate) (PMMA) as the shell, on the fracture properties of UP resins during curing. The focus is on the effects of the chemical composition in the shell of the CSR and the content of the CSR added to the UP. On the basis of an integrated approach of measurements combining the static phase characteristics of a styrene (ST)/UP/CSR system, the reaction kinetics, the cured sample morphology, the glass-transition temperatures, and the fracture toughness, an in-depth elucidation of the experimental results is presented.

EXPERIMENTAL

Synthesis of the CSR tougheners

The CSRs, with PBA as the core and methyl methacrylate (MMA; Acros, Morris Plains, NJ) copolymerized with crosslinking agent ethylene glycol dimethacrylate (EGDMA; Acros) and various concentrations of glycidyl methacrylate (GMA; Acros) as the shell, were synthesized by two-stage soapless emulsion polymerizations[9–11] in a 2-L, five-

Correspondence to: Y.-J. Huang (yjhuang@ch.ntust.edu.tw).
Contract grant sponsor: National Science Council of the Republic of China; contract grant number: NSC91-2216-E-011-016.

Journal of Applied Polymer Science, Vol. 107, 939–950 (2008)

TABLE I
Recipes for the First Stage of the Reaction for Preparing the CSR Core

Ingredient	Weight (g)	Moles
BA	45	0.35
KPS	1.305	0.00483
Deionized H_2O	1215	—

necked, glass-vessel reactor immersed in a constant-temperature water bath. The first stage of the reaction, preparing the core, was carried out in a semibatch mode (at a monomer feed rate of 0.75 mL/min for 1 h) at 70°C for 2 h; potassium persulfate ($K_2S_2O_8$ or KPS; Acros) was employed as an initiator, the weight ratio of water to the monomer was kept at 27 : 1, and a stirring speed of 450 rpm and a nitrogen sparge rate of 70 mL/min were employed. The prepared PBA core was then used as a seed for the second stage of the reaction, preparing the shell, which was carried out in a batch mode at 70°C for 2 h with KPS as an initiator. Before the second stage of the reaction, 12 h was allowed for the shell monomers to swell the seed. The recipes used for the synthesis of the four CSRs for this study are summarized in Tables I and II.

The properties of the four series of CSRs synthesized in this study, including butyl acrylate (BA)/MMA–EGDMA (the G0 type), BA/MMA–EGDMA–GMA(5) (the G1 type), BA/MMA–EGDMA–GMA(10) (the G2 type), and BA/MMA–EGDMA–GMA(16) (the G3 type), are summarized in Table III.

UP resins

The UP resins[12] were made from maleic anhydride (MA), 1,2-propylene glycol (PG), and phthalic anhydride (PA) with a molar ratio (MR) of 0.62 : 1.25 : 0.38. The acid number and hydroxyl number were found to be 29.4 and 31.0 by end-group titration, which gave a number-average molecular weight of 1858 g/mol. On average, there were 5.95 C=C bonds per UP molecule.

Preparation of the sample solutions

For the sample solutions, 0, 5, or 10 wt % CSR was added, whereas the MR of ST to polyester C=C bonds was fixed at 2 : 1. The reaction was initiated by 1 wt % *tert*-butyl perbenzoate. All the cure reactions were carried out at 110°C isothermally for 1 h, and they were followed by a postcure at 150°C for another hour.

Phase characteristics

To study the compatibility of the ST/UP/CSR systems before the reaction, 20-g sample solutions were prepared in 100-mL separatory glass cylinders, which were placed in a constant-temperature water bath at 30 or 110°C. The phase-separation time and relative weights of the upper and bottom layers were recorded. For the experiment at 110°C, 0.25 wt % benzoquinone was added as an inhibitor to prevent crosslinking reactions during the experiment.

Cure kinetics

For the study of the cure kinetics, a 6–10-mg sample solution was placed in a hermetic aluminum sample pan. The isothermal reaction rate profile at 110°C was measured with a DuPont 9000 differential scanning calorimeter (TA Instruments, New Castle, DE), and the final conversion of total C=C bonds at 110°C was calculated.[13]

Scanning electron microscopy (SEM)

The sample solutions were degassed in a vacuum oven at 50°C for 5 min and were then slowly poured into stainless steel rectangular molds with inner trough dimensions of 17 × 1.7 × 0.42 cm^3 and sealed with gaskets. The sample solutions were cured at 110°C in a thermostated silicon oil bath for 1 h, and this was followed by a postcure at 150°C for another hour.

In the morphological study, the cured sample in the mold was removed and broken into several

TABLE II
Recipes for the Second Stage of the Reaction for Preparing the CSR Shell

CSR code	Simple code	MMA (g)	GMA (g)	EGDMA (g)	KPS (g)
BA/MMA–EGDMA	G0	43.52	0	0.315	0.315
BA/MMA–EGDMA–GMA(5)	G1	40.35	3.15	0.315	0.315
BA/MMA–EGDMA–GMA(10)	G2	37.16	6.33	0.315	0.315
BA/MMA–EGDMA–GMA(16)	G3	34.02	9.49	0.315	0.315

A stirring speed of 450 rpm and a nitrogen sparge rate of 70 mL/min were employed for the second stage of reaction.

TABLE III
CSRs Used in this Study

CSR code	Simple code	Monomers	Molar composition of the monomers	T_g (C)[a] Low	Medium	High	D_n (nm)[b]
BA/MMA–EGDMA	G0	Core: BA Shell: MMA, EGDMA	Core: 0.811 Shell: 0.996:0.004	−57.0	—	108.1	229.8
BA/MMA–EGDMA–GMA(5)	G1	Core: BA Shell: MMA, EGDMA, GMA	Core: 0.826 Shell: 0.944:0.004:0.052	−50.3	−19.4	116.8	230.4
BA/MMA–EGDMA–GMA(10)	G2	Core: BA Shell: MMA, EGDMA, GMA	Core: 0.841 Shell: 0.889:0.004:0.107	−49.7	−15.9	118.8	223.6
BA/MMA–EGDMA–GMA(16)	G3	Core: BA Shell: MMA, EGDMA, GMA	Core: 0.857 Shell: 0.833:0.004:0.164	−50.4	−16.6	115.0	230.9

[a] Glass-transition temperature by DSC. The low, medium, and high values are those of the core (i.e., PBA), interlayer (i.e., PBA-*g*-PMMA), and shell (i.e., lightly EGDMA-crosslinked PMMA) of the CSR, respectively.
[b] By TEM.
D_n, number-average diameter of the CSR.

pieces. After the usual sample pretreatment,[14] a Hitachi S-550 scanning electron microscope (Pleasanton, CA) with an accelerating voltage of 20 kV was used to observe the fractured surface of each sample at magnifications of 1000–5000×.

Transmission electron microscopy (TEM)

TEM images of the cured samples were obtained at 80 kV with a JEOL 1200 EX II transmission electron microscope (Tokyo, Japan). The samples were ultramicrotomed with a glass knife on a Reichert-Jung Ultracut E microtome (Wetzlar, Germany) at room temperature to make sections approximately 80 nm thick. The sections were transferred from the knife edge to 200-mesh Cu girds, and this was followed by staining in a 1 wt % OsO_4 solution for 1 day, washing with water to remove the excess of OsO_4 on the samples, and drying at the ambient temperature for 1 day.

Mechanical and fracture properties

In the mechanical tests, dumbbell-shaped specimens based on ASTM D 638-82a type V were used to determine the tensile properties of cured polyester matrices on a Micro 350 universal testing machine (Testometric Co., Lancashire, United Kingdom) at a constant crosshead speed of 1.0 mm/min. The Izod impact test was carried out on the basis of ASTM D 256-81 method A with an impact tester (Frank pendulum impact tester model 53568, Zwick, Ulm, Germany).

Tests of the fracture mechanics were carried out on sharply notched three-point-bending specimens based on ASTM E 399-83-A3 with a crosshead speed of 1 mm/min. The fracture toughness (K_{IC}) and the fracture energy (G_{IC}) were then calculated with the following equations:

$$K_{IC} = P_Q S/(BW^{3/2}) f(a/W) \quad (1)$$

$$f(a/W) = 3(a/W)^{1/2}[1.99 - a/W(1-a/W)(2.15 - 3.93a/W + 2.7a^2/W^2)]/[2(1+2a/W)(1-a/W)^{3/2}] \quad (2)$$

$$G_{IC} = K_{IC}{}^2(1-\nu^2)/E \quad (3)$$

where P_Q is the maximum load, B is the sample thickness, S is the support span, W is the sample width, a is the initial crack length, ν is Poisson's ratio, and E is Young's modulus. Both ν and E values were obtained from tensile tests.

Thermally stimulated current (TSC) method

For the measurements of the transition temperatures in each phase region of the cured ST/UP/CSR systems, a sample specimen with a thickness of 1.0 mm was polarized at 150°C under an electric field of 120 V/mm over a period of 0.01 min with a Solomat (Stamford, CT) 91000 TSC/relaxation map analysis apparatus.[15,16] TSCs were recorded from −100 to 250°C at a heating rate of 7°C/min. For neat CSR samples, each sample in a powder form was pressed under 500 psi for 5 min to make a disk for the subsequent TSC testing. A sample specimen with a thickness of 1 mm was polarized at 130–150°C under the same electric field and over the same polarization time period used for the ST/UP/CSR systems.

RESULTS AND DISCUSSION

Compatibility of the ST/UP/CSR systems

The solubility parameter is a compatibility criterion generally accepted for polymeric mixtures and solu-

TABLE IV
Molar Volumes, Cohesive Energies, and Solubility Parameters for UP, ST, and the CSR Shell

UP or CSR shell		Molar volume (cm^3/mol)	Cohesive energy (J/mol)	Solubility parameter $(J^{1/2}/cm^{3/2})^b$	Solubility parameter for the CSR shell − solubility parameter for ST/UP $(J^{1/2}/cm^{3/2})$
UP resin and ST	MA–PG–PA type of UP	1468	678,200	21.49	
	ST	113.4	40,560	18.91	
	ST/UP mixture (MR = 2/1)			20.25[c]	—
Shell of CSR	MMA–EGDMA	82.27[a]	34,010[a]	20.33	0.08
	MMA–EGDMA–GMA(5)	89.46[a]	37,810[a]	20.56	0.31
	MMA–EGDMA–GMA(10)	97.85[a]	42,230[a]	20.78	0.53
	MMA–EGDMA–GMA(16)	107.7[a]	47,440[a]	20.99	0.74

[a] Based on one repeating unit of the polymer.
[b] (Cohesive energy/Molar volume)$^{1/2}$.
[c] $\delta_{mixture} = \Sigma\phi_i\delta_i$, where $\delta_{mixture}$ is the solubility parameter for the mixture, ϕ_i is the volume fraction of species i, and δ_i is the solubility parameter of species i.

tions in technological and scientific activities. The calculated solubility parameters for the UP resin, ST monomer, and the CSR shell, based on the cohesive energy and the molar volume for constitution unit i of the species, as suggested by Fedors,[17,18] are listed in Table IV. In general, the higher the difference was in the solubility parameters of the ST/UP mixture and the CSR shell, the lower the compatibility was for the ST/UP/CSR system at 30°C before the reaction. (In the preparation of the ST/UP/CSR ternary system, CSR was first swollen in the ST monomer for 1 day at room temperature, and this was followed by the addition of the UP resin and the high-shear mixing of the ternary mixture for 20 min at 60°C.) The data in Table IV reveal that adding a CSR with a higher amount of the relatively polar monomer GMA in the shell versus one with the relatively nonpolar monomer MMA (the monomer ST was less polar than the monomer MMA) led to lower compatibility of the ST/UP/CSR ternary system. Among the four ST/UP/CSR systems, a sample solution containing BA/MMA–EGDMA–GMA(16) (i.e., the G3 system) would theoretically be the least compatible, followed by the BA/MMA–EGDMA–GMA(10) (i.e., G2), BA/MMA–EGDMA–GMA(5) (i.e., G1), and BA/MMA–EGDMA (i.e., G0) systems. This is generally in agreement with the static phase characteristic data for the uncured ST/UP/CSR systems at 30 and 110°C (Table V): the G3-type CSR could not dissolve in ST/UP mixtures to form an ST/UP/10% CSR solution. Also, the degree of phase separation, as revealed by the weight ratio of the lower and upper layer solutions, was greatest for the G2 system (the ratio was closest to 1), which was followed by the G1 and G0 systems. Table V also shows that as the mixing temperature of the ST/UP/CSR ternary systems increased from 30 to 110°C, a higher degree of phase separation (i.e., the weight ratio of lower and upper layer solutions was closer to 1) and a shorter phase-separation time resulted. For the G0 system,

TABLE V
Phase-Separation Characteristics for ST/UP/10% CSR Uncured Systems at 30 and 110°C and Final Conversions of the Total C=C Bonds as Measured by DSC for ST/UP/10% CSR Systems Cured at 110°C

CSR added	Simple code	Phase-separation time at 30°C (min)	Relative weight of the lower layer at 30°C (%)	Phase-separation time at 110°C (min)	Relative weight of the lower layer at 110°C (%)	Final cure conversion of the total C=C bonds at 110°C (%)[a]
Neat UP						83.2
CSR						
BA/MMA–EGDMA	G0	2160	24	1800	26	78.5
BA/MMA–EGDMA–GMA(5)	G1	180	28	40	32	85.3
BA/MMA–EGDMA–GMA(10)	G2	80	33	25	37	85.0
BA/MMA–EGDMA–GMA(16)[b]	G3					

[a] Measured by DSC.
[b] The G3-type CSR could not dissolve in ST/UP mixtures to form a ST/UP/10% CSR solution at 30 or 110°C.

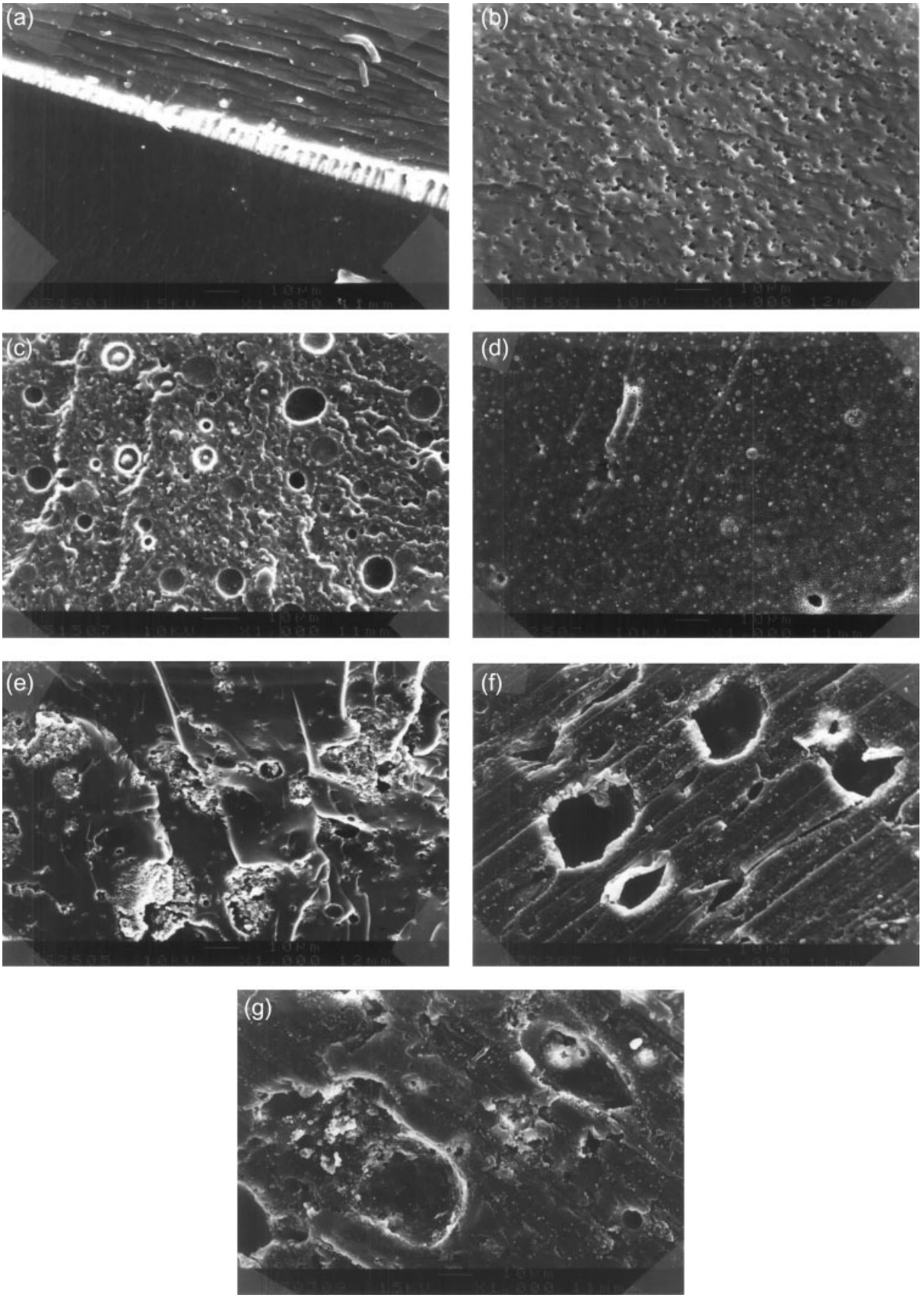

Figure 1 Effects of the CSR types and concentrations on the morphology of cured ST/UP/CSR samples at MR = 2 : 1 under SEM: (a) neat UP, (b) 5% G0, (c) 10% G0, (d) 5% G1, (e) 10% G1, (f) 5% G2, and (g) 10% G2.

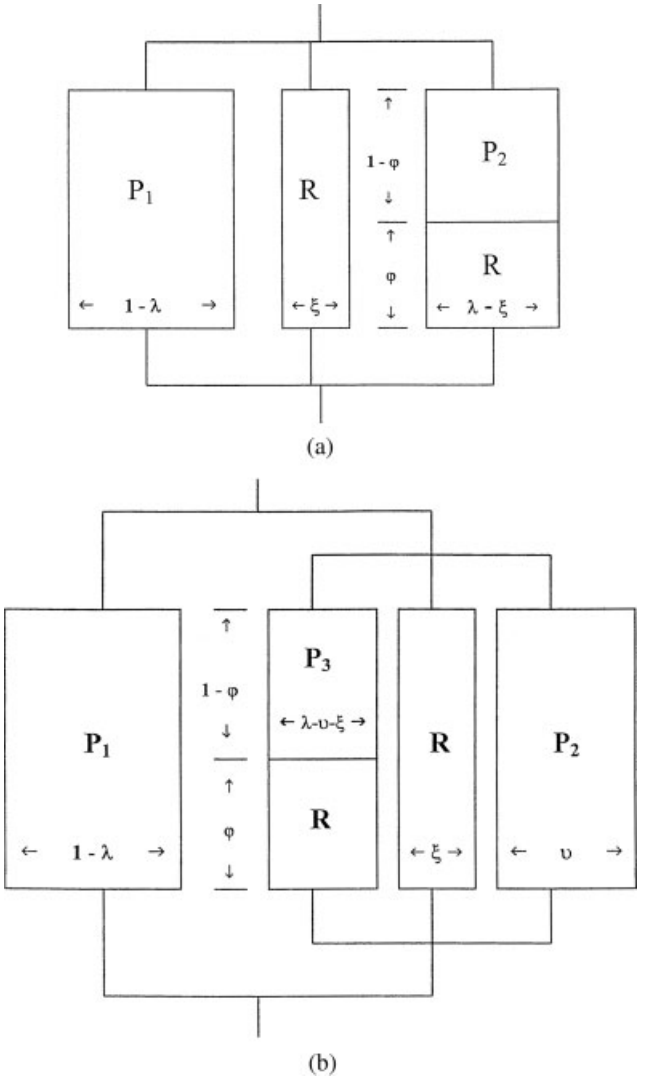

Figure 2 Takayanagi models for the mechanical behavior of cured CSR-containing UP resin systems: (a) P–P–S model and (b) P–(P–P–S) model. The area of each diagram is proportional to the volume fraction of the phase.

the phase-separation time at 110°C was still greater than 24 h, which was in contrast to a phase-separation time of less than 60 min for the G1 and G2 systems. Because the cure time for the ST/UP/CSR system at 110°C was within 90 min in this work, it was inferred that for the G0 system, the phase separation would be least noticeable during the cure at 110°C, whereas it would be more pronounced for the G1 and G2 systems.

During the cure at 110°C, SEM micrographs showed that the sample solution containing no CSR exhibited a flakelike microstructure [Fig. 1(a)]. Adding a CSR at either a 5 or 10 wt % level caused a less compatible ST/UP/CSR system with a two-phase microstructure, which consisted of a flakelike continuous phase and a CSR-dispersed phase [Fig. 1(b–g)]. At a fixed CSR content, the G0 system was the least incompatible, as evidenced by the smallest average area for the dispersed phase, followed by the G1 system and the G2 system, which showed the same trend for compatibility as the uncured ST/UP/CSR systems (Table V). For a fixed type of CSR, adding a larger amount of CSR may lead to more incompatibility of the ST/UP/CSR system, again as evidenced by the larger average area for the CSR-dispersed phase.

Relationship between the morphology and mechanical properties: the Takayanagi models

For the cured CSR-containing UP resin systems with characteristic morphologies, the mechanical behavior can be approximately represented by the Takayanagi models,[19,20] in which arrays of weak CSR (R) and stiff ST-crosslinked polyester (P) phases are employed (Fig. 2). For all six ST/UP/CSR systems, in which the CSR was about 230 nm in diameter and the shell material of the CSR was relatively nonpolar in comparison with the UP matrix, the two-phase microstructure can be represented by a parallel–parallel–parallel–series [P–(P–P–S)] model [Fig. 2(b)]. In contrast, for the ST/UP/LPA system containing poly (vinyl acetate) as an LPA, a homogeneous globule morphology may arise,[21] which can be represented by a parallel–parallel–series (P–P–S) model [Fig. 2(a)]. A similar globular morphology for the ST/UP/CSR cured system would be observed if the shell material of the CSR were composed of relatively polar poly(vinyl acetate).

Effects of drift in the ST/polyester composition during curing on the cure kinetics

The isothermal differential scanning calorimetry (DSC) rate profiles (Fig. 3) revealed that adding a

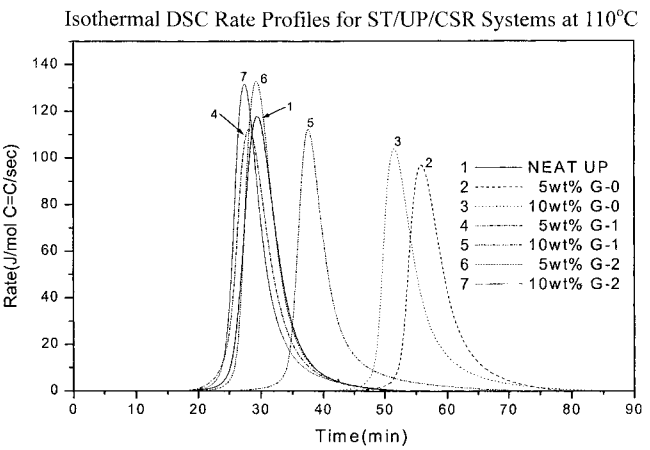

Figure 3 Effects of the CSR types and concentrations on the DSC reaction rate profile at 110°C for ST/UP/CSR systems.

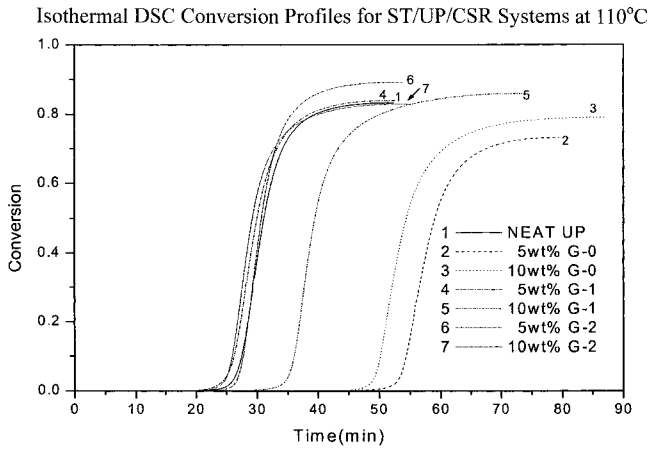

Figure 4 Effects of the CSR types and concentrations on the DSC reaction conversion profile at 110°C for ST/UP/CSR systems.

CSR generally delayed the onset of the cure reaction and reduced the maximum reaction rate at 110°C (except for the G2 systems, for which the maximum reaction rate increased). The induction time (i.e., inhibition time) was longest for the most compatible ST/UP/CSR system containing 5% G0 as the CSR. This was ascribed to the highest degree of swelling of the G0-type CSR by ST monomer and the MR of ST to polyester C=C bonds deviating most from (less than) 2 : 1 in the major continuous phase. (Our previous research showed that the reactivity of the ST/UP mixture would reach a maximum at MR = 2 : 1.[13] Decreasing MR from 2 : 1, during aggravation by the higher viscosity of the ST/UP mixture, could thus lead to an increase in the induction time.) Because of the lowest reactivity caused by the lowest MR in the major continuous phase, the maximum DSC reaction rate was the lowest for the most compatible ST/UP/5% G0 system. In addition, for the ST/UP/CSR systems, the most compatible ST/UP/5% G0 system exhibited the lowest final conversion of total C=C bonds (72.5%; see Fig. 4). This was because the lowest MR in the major continuous phase for the 5% G0 system resulted in the most compact microgel structure therein, leading to the lowest final conversion of total C=C bonds due to the lowest swelling effect of ST monomers on the microgel structures.[13]

Effects on CSR on the mechanical properties

The effects of CSR on the mechanical properties of the ST/UP/CSR systems are displayed in Table VI. Adding a CSR led to a decrease both in the impact strength (by 15–30%) and in the tensile strength (by 15–45%). For the ST/UP/CSR systems, both the impact strength and the tensile strength were the highest for the most compatible G0 system, which was followed by the G1 system and the least compatible G2 system. This was ascribed to the better interfacial adhesion for the more compatible ST/UP/CSR system. On the other hand, at a fixed CSR, adding a higher amount of the CSR could cause a decrease in the impact strength and the tensile strength because of the lower compatibility of the ST/UP/CSR system during the cure.

As for Young's modulus, it was increased by the addition of a CSR (by 3–16%) in comparison with the neat UP system, which showed a trend that was the reverse of those of the impact and tensile strengths. Also, Young's modulus was generally highest for the least compatible G2 system. At a fixed CSR, adding a larger amount of the CSR could cause an increase in the impact strength. On the basis of the isostrain model in Figure 2(a,b), Young's modulus of a sample would be dominated by $(1 - \lambda)E_{P1}$ (where E_{P1} is Young's modulus of the major continuous phase) because the moduli of phases R, P_2, and P_3 multiplied by their corresponding volume fractions would generally be much smaller than that of phase P_1 multiplied by its volume fraction [i.e., $(1 - \lambda)E_{P1}$]. Because Young's modulus represents the extent of resistance to deformation for a sample in the initial stage of a tensile test, during which the sample would be unbroken, it is connected to the degree of tightness of the network rather than the degree of crosslinking of the sample. For ST/UP/

TABLE VI
Mechanical Properties for the ST/UP/CSR systems After an Isothermal Cure at 110°C for 1 h and a Postcure at 150°C for Another Hour

CSR added	Impact strength (J/m)	Tensile strength (MPa)	Young's modulus (MPa)	Fracture toughness (MPa $m^{1/2}$)	Poisson's ratio	Fracture energy (kJ/m^2)
Neat UP	20.4(0.6)	26.6(2.3)	394(15)	1.09(0.02)	0.38(0.02)	2.58(0.23)
5 wt % G0	17.2(0.4)	22.7(1.2)	412(11)	1.61(0.02)	0.30(0.03)	5.58(0.39)
10 wt % G0	15.7(0.2)	19.4(1.3)	431(11)	1.34(0.02)	0.28(0.04)	3.84(0.31)
5 wt % G1	17.0(0.2)	20.3(1.1)	405(15)	1.32(0.01)	0.33(0.03)	3.83(0.28)
10 wt % G1	15.2(0.3)	18.5(1.5)	410(12)	1.26(0.02)	0.31(0.05)	3.50(0.34)
5 wt % G2	15.3(0.2)	15.6(1.1)	449(15)	1.30(0.01)	0.31(0.02)	3.35(0.20)
10 wt % G2	14.4(0.1)	14.8(1.5)	457(14)	1.24(0.01)	0.30(0.04)	3.01(0.22)

[a] The values in parentheses represent the estimated standard errors for the experimental averages.

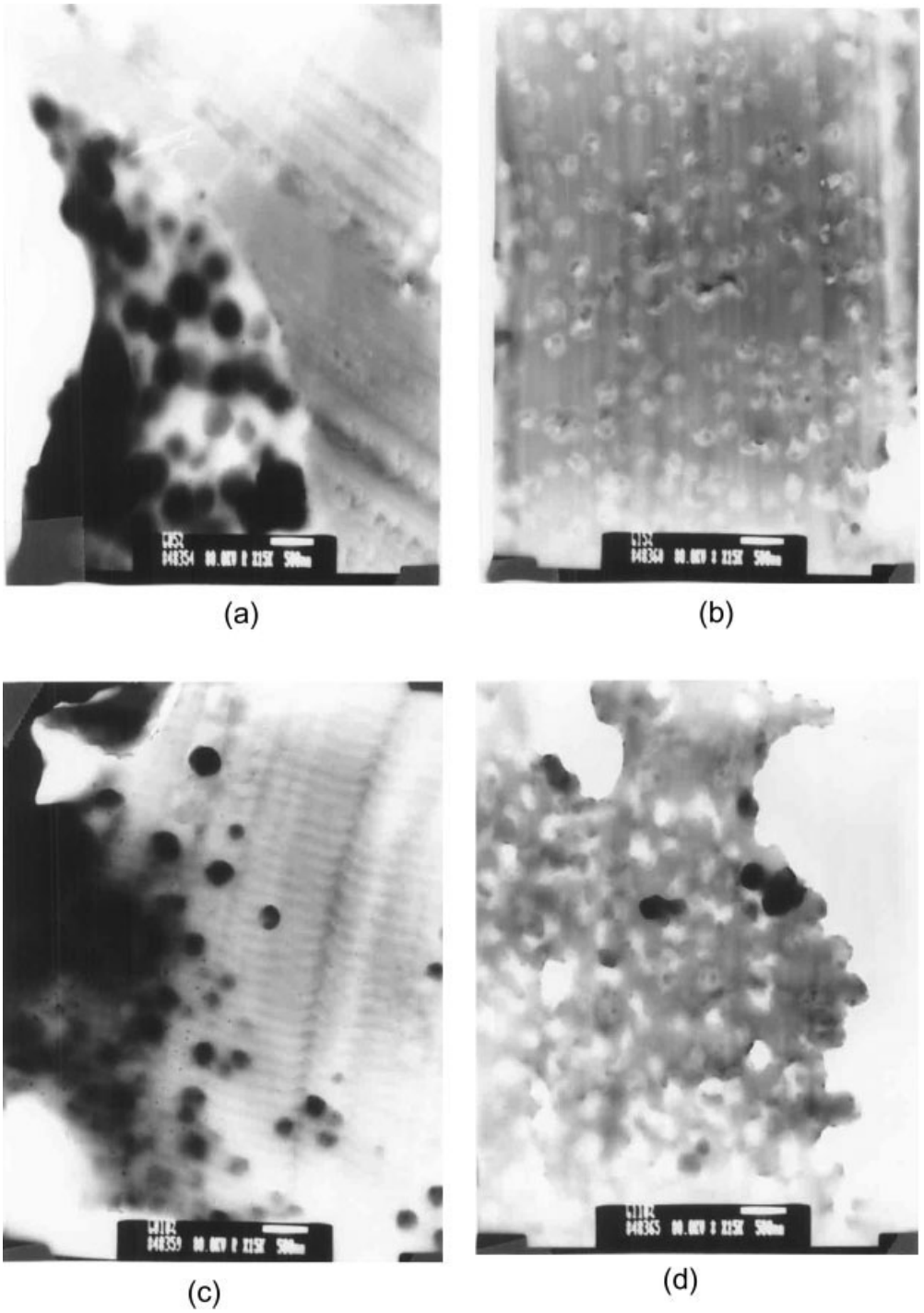

Figure 5 Effects of the CSR types and concentrations on the morphology of cured ST/UP/CSR samples at MR = 2 : 1 under TEM: (a) 5% G0, (b) 5% G1, (c) 10% G0, and (d) 10% G1.

CSR systems, a higher degree of phase separation during the cure may lead to a lower ST content in the continuous phase of a crosslinked polyester [phase P_1 in Fig. 2(a,b)]. A lower average crosslink length of ST and a more compact network in that phase may result after the cure, which, in turn, can lead to a higher value of Young's modulus for the whole sample.

For the fracture properties, adding a CSR would lead to an increase in both the fracture toughness (by 15–50%) and the fracture energy (by 15–115%); this shows a trend that is the reverse of that of the impact strength. For the ST/UP/CSR systems, both the fracture toughness and fracture energy were highest for the most compatible G0 system, which was followed by the G1 system and the least

compatible G2 system. This was ascribed to the better interfacial adhesion for the more compatible ST/UP/CSR system. On the other hand, at a fixed CSR, adding a larger amount of the CSR could cause a decrease in the fracture toughness and fracture energy because of the lower compatibility of the ST/UP/CSR system during the cure.

Toughening mechanism

As cited by Sue et al.,[22] for rubber-modified epoxy systems, an order of magnitude increase in the toughness is due to the cavitation of the rubber particles caused by the triaxial stress associated with the crack tip, followed by large-scale shear yielding of the epoxy matrix around the particles. For significant plastic shear banding to operate under constrained conditions in both thermoplastic and thermoset systems, cavitation of the toughener phase is essential via internal rubber particle cavitation, debonding at the interface, or a crazing mechanism. In other words, a sequence of toughening events (i.e., cavitation occurs first, followed by shear banding) and a causal relationship (i.e., without the cavitational process, the shear banding mechanism cannot take place) are involved in the toughening process.

For an ST/UP/CSR system containing a 5 wt % concentration of a G0-type CSR, a TEM micrograph (Fig. 5) revealed that CSR particles (0.25 μm in size) were coagulated locally as a cluster (with a size range of 0.5–1.5 μm) in the CSR-dispersed phase, and this was not observed for the other ST/UP/CSR systems. Sue et al.[22] reported that when CSR particles cluster locally, they can be mechanically treated as a large particle, and consequently, the crack-deflection mechanism can be enhanced;

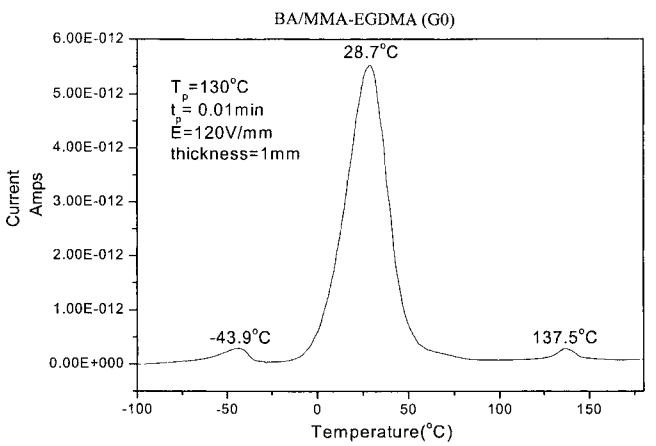

Figure 6 TSC profile for the G0-type CSR. The test conditions, including the polarization temperature (T_p) applied electric field (E), polarization time (t_p), and sample thickness, are indicated.

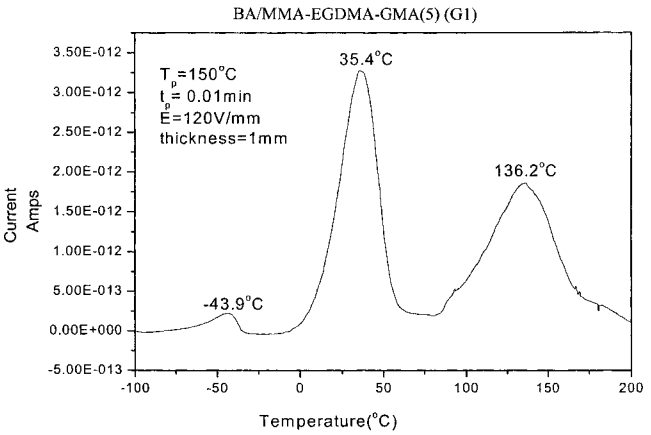

Figure 7 TSC profile for the G1-type CSR. The test conditions, including the polarization temperature (T_p) applied electric field (E), polarization time (t_p), and sample thickness, are indicated.

this leads to a great increase in the mechanical toughness.

Crosslinking density and diffusion effects of ST in CSR on the glass-transition temperature of the P phase

Figures 6 and 7 show the TSC profiles for two CSRs, G0 and G1, respectively; the glass-transition temperatures are identified and are listed in Table VII. Three glass-transition temperatures have been detected for each CSR: the low, medium, and high glass-transition temperatures are the glass-transition temperatures for the core (i.e., PBA), the interlayer (i.e., PBA-*g*-PMMA), and the shell (i.e., lightly EGDMA-crosslinked PMMA) of the CSR, respectively.

Figures 8 and 9–12 show the TSC profiles for the cured neat UP resins and the cured ST/UP/CSR systems, respectively; the glass-transition temperatures are identified and are listed in Table VIII. For the

TABLE VII
Glass-Transition Temperatures (°C) for Neat CSRs as Determined by the TSC Method

CSR code	Simple code	T_{g1CSR}[a]	T_{g2CSR}[b]	T_{g3CSR}[c]
BA/MMA–EGDMA	G0	137.5	28.7	−43.9
BA/MMA–EGDMA–GMA(5)	G1	136.2	35.4	−43.9
BA/MMA–EGDMA–GMA(10)	G2	—	—	—

[a] Glass-transition temperature for the shell (i.e., lightly EGDMA-crosslinked PMMA) of the CSR.
[b] Glass-transition temperature for the interlayer (i.e., PBA-*g*-PMMA) of the CSR.
[c] Glass-transition temperature for the core (i.e., PBA) of the CSR.

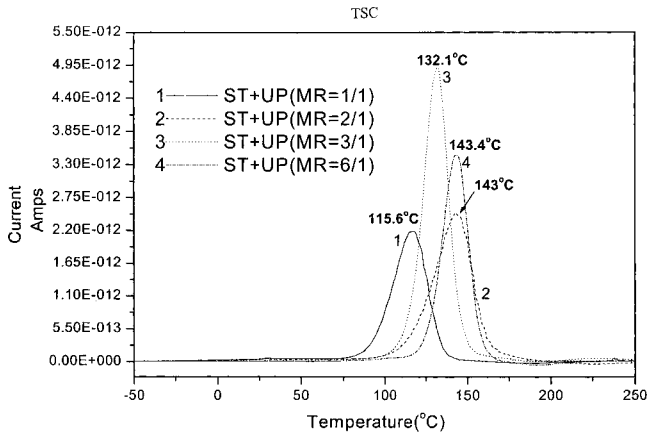

Figure 8 TSC profiles for cured neat UP resins at MR values of 1 : 1, 2 : 1, 3 : 1, and 6 : 1 after an isothermal cure at 110°C for 1 h and a postcure at 150°C for 1 h.

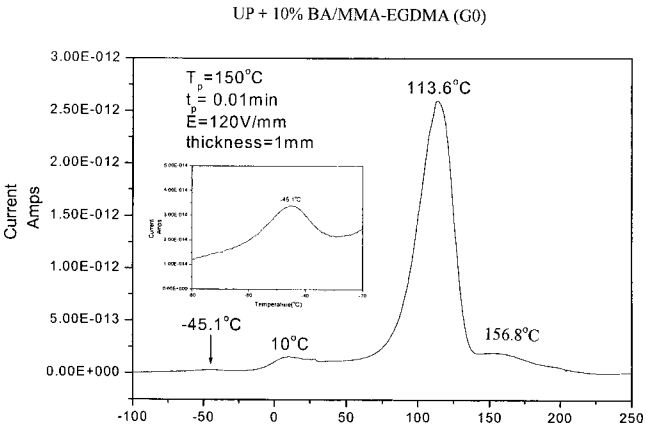

Figure 10 TSC profile for the cured ST/UP/10% G0 system at MR = 2 : 1 after an isothermal cure at 110°C for 1 h and a postcure at 150°C for 1 h. The test conditions, including the polarization temperature (T_p) applied electric field (E), polarization time (t_p), and sample thickness, are indicated.

neat UP resin system, T_{g1} can be identified as the glass-transition temperature for the overall ST-crosslinked polyester matrix. As the MR increased, T_{g1} generally exhibited an increase followed by a decrease, and it reached a maximum at MR = 2 : 1 (T_{g1} = 143.0°C); this shows a trend similar to those reported in the literature.[23] At MR = 6 : 1, it was inferred that phase separation occurred during the cure, leading to one phase region with MR close to 2 : 1 (glass-transition temperature = 143.4°C) and another phase region containing essentially polystyrene (glass-transition temperature = 105.0°C).

As mentioned earlier, for all of the ST/UP/CSR systems in this work, a P–(P–P–S) model [Fig. 2(b)] is proposed. The glass-transition temperatures listed in Table VIII for the ST/UP/CSR cured systems are as follows: T_{g1} is the glass-transition temperature for the major continuous phase of ST-crosslinked polyester [i.e., phase P_1 in Fig. 2(b)], T_{g2} is the glass-transition temperature for the major microgel particle phase within the CSR-dispersed phase [i.e., phase P_2 in Fig. 2(b)], T_{g3} is the glass-transition temperature for the CSR cocontinuous phase within the CSR-dispersed phase [i.e., phase P_3 in Fig. 2(b)], and T_{gCSR} is the glass-transition temperature of the CSR phase. For the ST/UP/CSR systems represented by a P–(P–P–S) model, T_{g2} cannot be clearly identified by TSC and may be superposed with T_{g1}. For the less compatible ST/UP/CSR systems containing G1-type CSR, T_{g3} can be identified. This, however, cannot be observed for the more compatible ST/UP/CSR systems containing G0-type CSR.

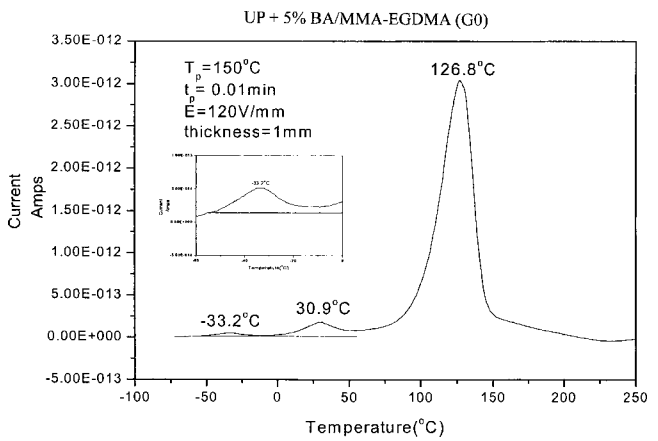

Figure 9 TSC profile for the cured ST/UP/5% G0 system at MR = 2 : 1 after an isothermal cure at 110°C for 1 h and a postcure at 150°C for 1 h. The test conditions, including the polarization temperature (T_p) applied electric field (E), polarization time (t_p), and sample thickness, are indicated.

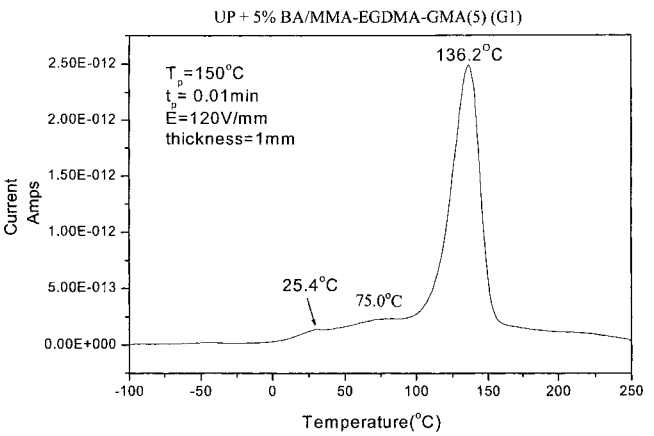

Figure 11 TSC profile for the cured ST/UP/5% G1 system at MR = 2 : 1 after an isothermal cure at 110°C for 1 h and a postcure at 150°C for 1 h. The test conditions, including the polarization temperature (T_p) applied electric field (E), polarization time (t_p), and sample thickness, are indicated.

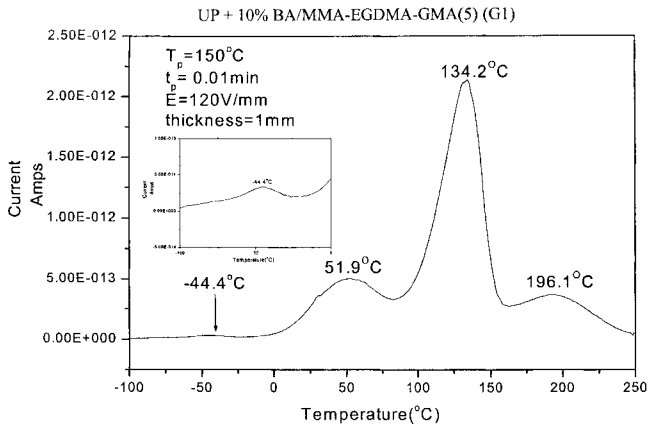

Figure 12 TSC profile for the cured ST/UP/10% G1 system at MR = 2 : 1 after an isothermal cure at 110°C for 1 h and a postcure at 150°C for 1 h. The test conditions, including the polarization temperature (T_p) applied electric field (E), polarization time (t_p), and sample thickness, are indicated.

The glass-transition temperature peaks at 156.8 and 196.1°C for the 10% G0 and 10% G1 systems, respectively (i.e., Figs. 10 and 12), were due to a local phase of high crosslinking density, which was generated during the TSC test, within the major continuous ST-crosslinked polyester phase. The heating from −100 to 250°C at a heating rate of 7°C/min during the TSC experiments caused unreacted C=C bonds, which were buried in the microgel structure of the original sample specimens, to experience a further crosslinking reaction. (In other words, the crosslinking density of the original sample was increased during the TSC test, and the glass-transition temperature exceeding 150°C, as measured by TSC in this work, was greater than the glass-transition temperature of the original sample specimens before the TSC test.)

The data in Table VIII reveal that adding CSR could lead to an appreciable reduction in T_{g1} of 6–30°C in comparison with the neat UP resin system at MR = 2 : 1 (113–137 vs 143°C). For the ST/UP/CSR systems, T_{g1} was lower for the more compatible ST/UP/G0 system than for the less compatible ST/UP/G1 system (113–127 vs 134–137°C). For a fixed CSR, the less compatible ST/UP/CSR system, caused by the addition of a larger amount of the CSR, resulted in a decrease in T_{g1}. This was because for the less compatible ST/UP/CSR cured system, the MR of consumed ST to reacted polyester C=C bonds deviated more from (less than) 2 : 1 in the major continuous phase (P_1), leading to a lower crosslinking density in that phase.

As mentioned earlier, because of the diffusion effect of ST monomers in the CSR for the ST/UP/CSR system, the ST concentration in the major continuous phase as a result of phase separation during the cure decreased. The highest degree of swelling of a G0-type CSR by ST monomers, due to the most compatible ST/UP/CSR system, resulted in the MR of ST to polyester C=C bonds (MR) deviating most from (less than) 2 : 1 in the major continuous phase during the cure. Hence, the glass-transition temperature in the P_1 phase for the cured ST/UP/CSR system was lower for the G0 system than for the G1 system (the glass-transition temperature in the P_1 phase reached a maximum at an MR of 2:1 for the cured UP resin system, for which the crosslinking density was the highest).

CONCLUSIONS

CSRs with PBA as the soft core and with MMA copolymerized with EGDMA and various concentrations of GMA as the hard shell can be used as toughers for UP resins. Adding such CSRs may lead to an increase both in the fracture toughness (by 15–50%) and the fracture energy (by 15–115%) in comparison with those of the neat UP resin system cured at 110°C.

Decreasing the content of GMA in the CSR shell can enhance the compatibility of an ST/UP/CSR system both before and during the cure reaction at 110°C. The former can be predicted by the calculated difference in the solubility parameters of the CSR shell and the ST/UP mixture with group contribu-

TABLE VIII
Glass-Transition Temperatures (°C) of the Fully Cured ST/UP/CSR Systems as Determined by the TSC Method

CSR		MR	Model	T_{g1} (°C)	T_{g2} (°C)	T_{g3} (°C)	T_{gCSR} (°C)
Neat UP		1/1		115.6			
		2/1		143.0			
		3/1		132.1			
		6/1		143.4	105.0		
CSR	5 wt % G0	2/1	P–(P–P–S)	126.8	—	—	30.9, −33.2
	10 wt % G0	2/1	P–(P–P–S)	113.6	—	—	10.0, −45.1
	5 wt % G1	2/1	P–(P–P–S)	136.2	—	75.0	25.4
	10 wt % G1	2/1	P–(P–P–S)	134.2	—	51.9	−44.4

tion methods. For the ST/UP/CSR system containing 5 or 10% CSR, the cured sample morphology showed a two-phase microstructure that consisted of a flakelike continuous phase and a CSR-dispersed phase. Its mechanical properties may be approximately represented by a P–(P–P–S) Takayanagi model.

In this work, the most compatible ST/UP/CSR system containing 5 wt % BA/MMA–EGDMA as a CSR (i.e., G0-type CSR containing no GMA in the shell) resulted in the best impact, tensile, and fracture properties among the six ST/UP/CSR systems, yet the glass-transition temperature in the major ST-crosslinked polyester phase showed an appreciable drop (16°C) in comparison with the neat UP resin system (glass-transition temperature = 143°C). For the ST/UP/5% G0 system, in addition to the best interfacial adhesion, CSR particles, coagulating locally as a cluster in the CSR-dispersed phase as observed from TEM micrographs, led to a crack-deflection mechanism for the facilitation of increasing mechanical toughness.

References

1. Burns, R. Polyester Molding Compounds; Marcel Dekker: New York, 1982.
2. Atkins, K. E. In Sheet Molding Compounds: Science and Technology; Kia, H. G., Ed.; Hanser: New York, 1993; Chapter 4.
3. B.F. Goodrich Co. PCT Int. Appl. WO93/21274 (1993).
4. Pandit, S. B.; Nadkarni, V. M. Ind Eng Chem Res 1994, 33, 2778.
5. Ullett, J. S.; Chartoff, R. P. Polym Eng Sci 1995, 35, 1086.
6. Abbate, M.; Martuscelli, E.; Musto, P.; Ragosta, G.; Scarinzi, G. J Appl Polym Sci 1995, 58, 1825.
7. Maspoch, M. L. L.; Martinez, A. B. Polym Eng Sci 1998, 38, 290.
8. Crc for Polymers Pty., Ltd. PCT Int. Appl. WO97/43339 (1997).
9. Lee, C. F.; Lin, K. R.; Chiu, W. Y. J Appl Polym Sci 1994, 51, 1621.
10. Lin, K. F.; Shieh, Y. D. J Appl Polym Sci 1998, 69, 2069.
11. Wu, J. H. M.S. Thesis, National Taiwan University of Science and Technology, 2003.
12. Huang, Y. J.; Jiang, W. C. Polymer 1998, 39, 6631.
13. Huang, Y. J.; Su, C. C. J Appl Polym Sci 1995, 55, 305.
14. Huang, Y. J.; Liang, C. M. Polymer 1996, 37, 401.
15. Huang, Y. J.; Lee, S. C.; Dong, J. P. J Appl Polym Sci 2000, 78, 558.
16. Ibar, J. P. Fundamentals of Thermal Stimulated Current and Relaxation Map Analysis; SLP: New Canaan, CT, 1993.
17. Krevelen, D. W. V. Properties of Polymers, 3rd ed.; Elsevier: London, 1990; p 196.
18. Fedors, R. F. Polym Eng Sci 1974, 14, 147.
19. Takayanagi, M.; Imada, K.; Kajiyama, T. J Polym Sci Part C: Polym Symp 1966, 15, 263.
20. Huang, Y. J.; Horng, J. C. Polymer 1998, 39, 3683.
21. Huang, Y. J.; Chen, T. S.; Huang, J. G.; Lee, F. H. J Appl Polym Sci 2003, 89, 3347.
22. Sue, H. J.; Garciameitin, E. I.; Pickelman, D. M. In Polymer Toughening; Arends, C. B., Ed.; Marcel Dekker: New York, 1996; Chapter 5.
23. Cook, W. D.; Delatycki, O. J Polym Sci Polym Phys Ed 1974, 12, 1925.